CHIN. PHYS. LETT. Vol. 37, No. 8 (2020) 080702

Characterization of Scanning SQUID Probes Based on 3D Nano-Bridge Junctions in Magnetic Field

Yin-Ping Pan(潘银萍)[1,2], Yue Wang(王悦)[1,3], Ruo-Ting Yang(杨若婷)[1,3], Yan Tang(汤演)[1], Xiao-Yu Liu(刘晓宇)[1], Hua Jin(金华)[1], Lin-Xian Ma(马林贤)[1], Yi-Shi Lin(林一石)[2], Zhen Wang(王镇)[1,3], Jie Ren(任洁)[1,3*], Yi-Hua Wang(王熠华)[2,4*], and Lei Chen(陈垒)[1,3*]

[1]*Center for Excellence in Superconducting Electronics, Shanghai Institute of Microsystem and Information Technology, Chinese Academy of Sciences, Shanghai 200050, China*
[2]*Department of Physics and State Key Laboratory of Surface Physics, Fudan University, Shanghai 200438, China*
[3]*University of Chinese Academy of Sciences, Beijing 100049, China*
[4]*Shanghai Research Center for Quantum Sciences, Shanghai 201315, China*

(Received 20 March 2020; accepted 24 June 2020; published online 28 July 2020)

We develop superconducting quantum interference device (SQUID) probes based on 3D nano-bridge junctions for the scanning SQUID microscopy. The use of these nano-bridge junctions enables imaging in the presence of a high magnetic field. Conventionally, a superconducting ground layer has been employed for better magnetic shielding. In our study, we prepare a number of scanning SQUID probes with and without a ground layer to evaluate their performance in external magnetic fields. The devices show the improved magnetic modulation up to 1.4 T. It is found that the ground layer reduces the inductance, and increases the modulation depth and symmetricity of the gradiometer design in the absence of the field. However, the layer is not compatible with the use of the scanning SQUID probe in the field because it decreases its working field range. Moreover, by adding the layer, the mutual inductance between the feedback coil and the SQUID also decreases linearly as a function of the field.

PACS: 07.79.−v, 85.25.−j DOI: 10.1088/0256-307X/37/8/080702

Recent advances in scanning superconducting quantum interference device (SQUID) microscopy[1−6] have contributed considerably to research of vortex dynamics, microscopic magnetism, and edge transport of topological states of matter.[6−11] Furthermore, observations of many exotic phenomena, such as the quantum Hall state[12,13] of quantum materials, require a high external magnetic field. We have developed a multi-functional Nb scanning SQUID probe based on 3D nano-bridge junctions, applied in scanning magnetometry, susceptometry, and current magnetometry up to a 0.5 T external magnetic field.[14] Conventionally, a superconducting ground layer is considered better at magnetic shielding of SQUIDs.[15,16] Therefore, a ground layer was added to our original device design[17] to enhance its performance in the magnetic field. In the present study, we prepared a number of SQUIDs with and without the ground layer to evaluate the influence of each on the functioning of devices, particularly in an external magnetic field. It is found that the ground layer in the scanning SQUID probe is actually not compatible in applications with such fields. The devices without the ground layer show the improved magnetic modulation up to 1.4 T, which shall broaden the study on many quantum materials.

The ground layer structure of each device [inset in Fig. 1(a)] is a 120-nm-thick Nb film and was first deposited on a Si substrate coated with 300 nm SiO_2. Then, the SQUID was fabricated following the protocol described in our previous paper.[17] The circuit of the SQUID [Fig. 1(a)] includes a pickup coil of 2 μm in diameter with counter-wound loops[18] that receive only the local magnetic signal from the sample without picking up any ambient uniform magnetic field. The length of SQUIDs was 0.5 mm, and the width is 1 μm. The modulation coil is coupled to the SQUID to generate a magnetic flux and locks the working point in the feedback mode while it is scanning. The field coil generates a small magnetic field in the portion of the sample closest to the tip. At the other end of the pick-up coil, the field coil with its symmetric structure generates a field of the same strength that compensates for the other. The SQUID consists of two 3D

Supported by the National Key R&D Program of China (Grant Nos. 2017YFF0206105, 2016YFA0301002 and 2017YFA0303000), the Young Investigator Program of CAS (Grant No. 2016217), the Frontier Science Key Programs of the CAS (Grant No. QYZDY-SSW-JSC033), and the Strategic Priority Research Program of CAS (Grant No. XDA18000000), the Shanghai Municipal Science and Technology Major Project (Grant No. 2019SHZDZX01), and the National Natural Science Foundation of China (Grant No. 11827805).
*Corresponding author. Email: jieren@mail.sim.ac.cn; wangyhv@fudan.edu.cn; leichen@mail.sim.ac.cn
© 2020 Chinese Physical Society and IOP Publishing Ltd

nano-bridge junctions[14,17] [Fig. 1(b)], fabricated by electron-beam lithography that allows the fine tuning of the thickness and width of nano-bridges. Also, in the ground layer, holes of 4 μm in diameter were patterned concentric with the field coil and modulation coil.

Two settings allow the modulation coil to apply a magnetic flux [Fig. 1(a)]. One sets the current flow from port 3 to port 4 (black arrows), with port 5 an open circuit; the other sets the current flowing from port 3 to ports 4 and 5 (orange arrows). The voltages of the SQUID were measured as a function of the applied current [Fig. 1(c), black and orange lines]. The current corresponding to a single flux quantum was 0.2 mA and 0.4 mA for the two mode settings, which allow one more adjustable level in the flux locking mode. Again, because of the symmetric structure, the flux generated by the field coil at one end of the pick-up coil compensates for the other by setting the current flowing from port 8 to port 6 [Fig. 1(a), red arrows]. This flux can also be measured by setting the current flowing from port 8 to port 7 [Fig. 1(a), blue arrows]. The voltage as a function of applied current [Fig. 1(d)] was plotted for SQUIDs (top) with and (bottom) without the ground layer; the current flows from port 8 to 7 and port 8 to 6 are presented as blue and red curves, respectively. A comparison of these curves establishes the symmetry of the device. Apparently, the device with a ground layer is more symmetric than the one without a ground layer caused most probably by the holes in the ground layer constricting the magnetic field inside; the effective area of the holes is better defined than the pick-up loop. In addition, the current flowing from port 8 to port 7 will apply a flux bias to the SQUID loop. It requires 5-mA current to generate one flux quanta in the SQUID loop with the ground layer, whereas 1 mA is required for the SQUID without the ground layer. The mutual inductance of the field coil to one end of the SQUID pickup loop with the ground layer is smaller, as is expected.

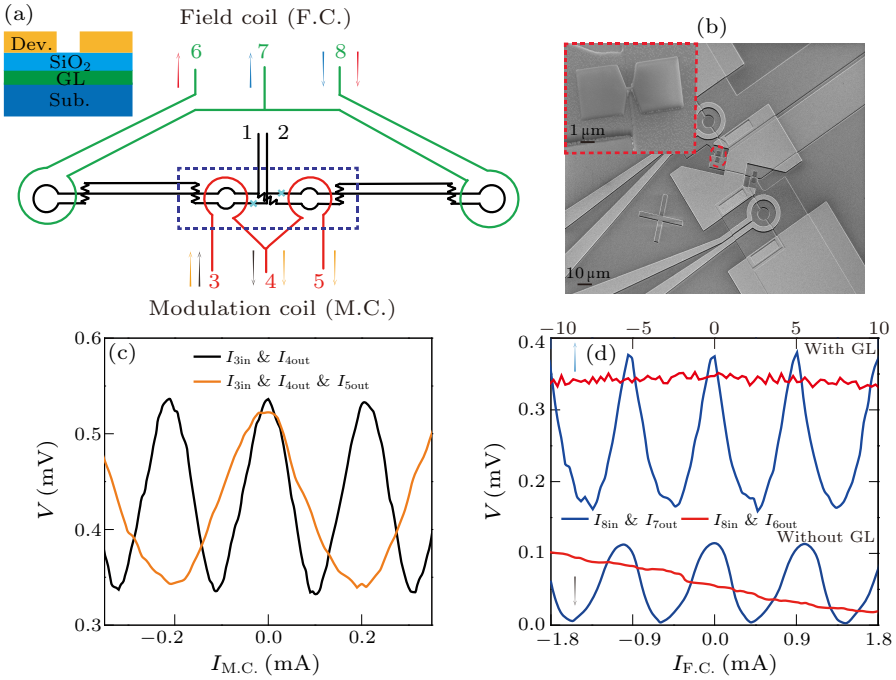

Fig. 1. (a) Circuit diagram of the scanning SQUID probe. The inset shows the layer structure of the device. (b) SEM image of the purple-dotted rectangle area in (a), with inset showing a zoomed-in view of the 3D nano-bridge junction. (c) Voltage of the SQUID as a function of applied current in the modulation coil for the two connecting modes. (d) Voltage of the SQUID as a function of applied current in the field coil for the two connecting modes. The two top curves correspond to a device with a ground layer; the two bottom curves corresponding to the one without a ground layer.

Four batches of SQUIDs with the same layout design were characterized at 4.2 K. The ground layers are absent in batches 1 and 2 (open squares and circles, respectively) and present in batches 3 and 4 (solid squares and circles, respectively). The normal resistance R_n is plotted [Fig. 2(a)] as a function of $1/I_c$. Here I_c denotes the critical current, and R_n the resistance of the SQUID in the normal state measured with a bias current greater than I_c. Theoretically, $R_n = \rho l j_c / I_c$, with ρ being the resistivity of niobium, l the effective length of the nano-bridge junction, and j_c the critical current density of the junction. Therefore, I_c should scale linearly with $1/R_n$ [Fig. 2(a)] with the same design size and materials for

our nano-bridges. However, with the points scattered over the diagram, no obvious linear scaling behavior is evident. Therefore, there is an uncertainty in either the effective length or the critical current density. We believe that the uncertainty comes from the size of the 3D nano-bridge junctions, which was affected by the randomness of the lift-off step during fabrication. In this case, the uncertainty may be decreased by finding a way to control the size of the junctions. However, the uncertainty can also arise from other more intrinsic properties of the Josephson effect in the 3D nano-bridge junction, such as the dependency of the critical current density j_c.

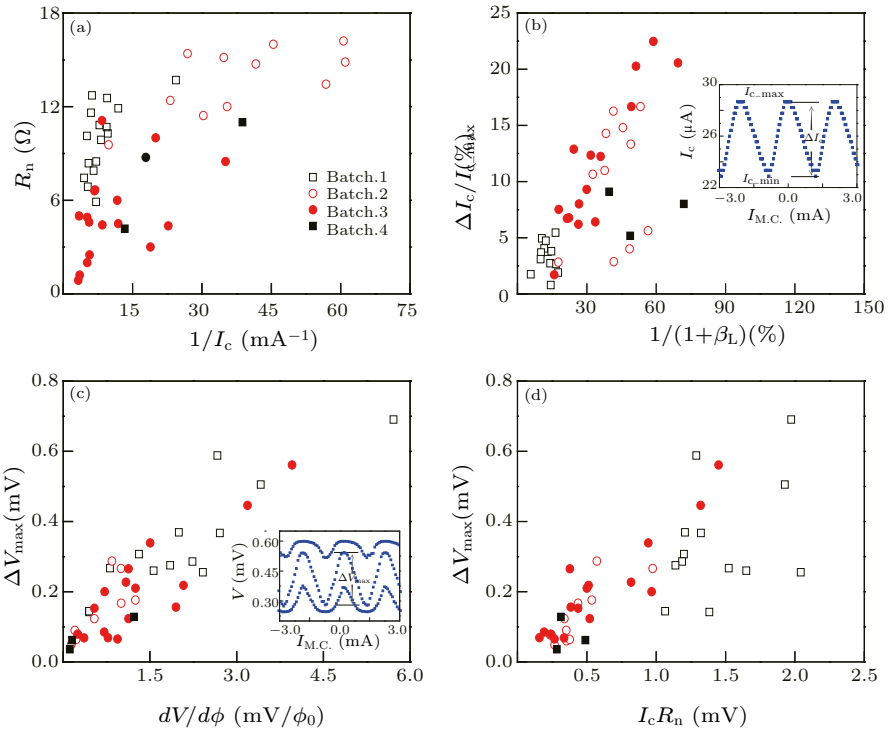

Fig. 2. Characterization of the four batches of scanning SQUID probes. Represented by open squares and circles, respectively, batches 1 and 2 have no ground layer. Batches 3 and 4, represented by solid squares and circles, respectively, have a ground layer: (a) normal resistance R_n of the SQUID as a function of reciprocal critical current I_c; (b) modulation depth of the SQUIDs as a function of the screening parameter (inset shows the modulation curves of a SQUID), (c) maximum voltage swing amplitude ΔV_{max} as a function of maximum differential voltage of the flux curves (inset shows voltage to the flux curves at various bias currents), and (d) maximum amplitude ΔV_{max} as a function I_cR_n.

We also measured the modulation depth $\Delta I_c/I_{c,max} = (I_{c,max} - I_{c,min})/I_{c,max}$ of our devices. Here I_c denotes the critical current at zero magnetic field; $I_{c,max}$ and $I_{c,min}$ are indicated in the inset of Fig. 2(b). The modulation depth shows rough linear scaling behavior with the screening parameter $1/(1+\beta_L)$ ($\beta_L = 2\pi I_c L_{SQUID}/\Phi_0$) as expected for SQUIDs. Here, L_{SQUID} denotes the SQUID inductance given by the simulation in InductEx[19,20] with the London penetration depth $\lambda_{Nb} = 110$ nm.[21] We obtained $L_{SQUID} = 38$ pH and 110 pH for SQUIDs with and without the ground layer, respectively. During microscopy scanning, we used a room-temperature preamplifier to read the voltage across the SQUID. Therefore, $dV/d\Phi$ and ΔV_{max} of the SQUIDs are two important parameters for read-out electronics. ΔV_{max} and $dV/d\Phi$ are, respectively, the maximum swing amplitude and the maximum differential voltage corresponding to the magnetic flux curves [see the inset of Fig. 2(c) at the optimal bias current],[22] $dV/d\Phi$ shows rough linear behavior as a function of ΔV_{max}. In addition, ΔV_{max} roughly increases linearly with I_cR_n [Fig. 2(d)]. By simply tuning the I_cR_n, a guiding rule is provided to fabricate the best-performing SQUID fitting our read-out electronics. Furthermore, no significant difference was observed from the SQUIDs with and without the ground layers (Fig. 2). Although the inserted ground layer decreases the inductance of a SQUID, a more important role arises that relies on a better control of the critical current of the 3D nano-bridge, which is unaffected by the ground layers.

The 3D nano-bridge junctions work in the presence of a high magnetic field.[23,24] We measured their resistance R as a function of temperature and magnetic field of the SQUIDs with and without the ground layer (Figs. 3(a) and 3(b)). The measurements were performed in a dry PPMS system with a rotational

sample puck. For both types, the critical magnetic field decreases to zero as temperature increases. The stop temperature for the zero critical field for SQUIDs with and without the ground layer are 6.5 K and 8.8 K, respectively. The critical fields for zero resistance at 2.0 K were 1.6 T and 1.7 T for SQUIDs with and without the ground layer, respectively. However, the field spreading region from 0 to 60 Ω is wider for the SQUIDs with a ground layer. The original assumption that the ground layer providing some magnetic shielding to the SQUIDs was confirmed.

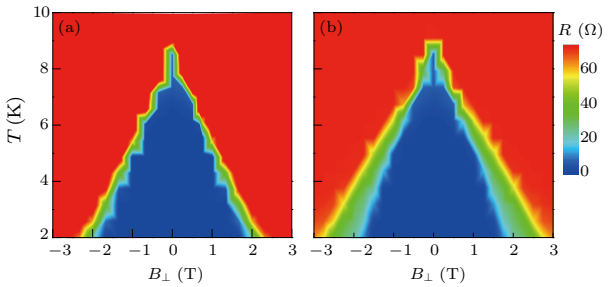

Fig. 3. Resistance of SQUID without (a) and with (b) the ground layer as versus temperature and magnetic field.

However, measurements of R_n cannot determine the performance of the SQUID because I_c does not show any obvious dependence on R_n. Therefore, we further investigated ΔV_{max} at various external magnetic fields (Fig. 4). The values of ΔV_{max} drops to zero by increasing the magnetic field for SQUIDs with or without the ground layer. It is indicated that the magnetic field suppresses the modulation performance of the SQUID. The open and solid black squares (red triangles) plot the maximum voltage swing ΔV_{max} of the SQUIDs without and with the ground layer, respectively, in various parallel (vertical) magnetic fields. The ΔV_{max} of the device without the ground layer drops to zero at 1.4 T and 1 T for the parallel and perpendicular magnetic field, respectively. The ΔV_{max} of the device with the ground layer drops to zero at 0.9 T and 0.8 T for the parallel and perpendicular magnetic fields, respectively. Moreover, ΔV_{max} drops slower in parallel fields than in vertical fields because the niobium film has a higher parallel critical magnetic field. Here the parallel magnetic field probably still has ∼5° uncertainty offset from the SQUID plane. The ΔV_{max} of a SQUID with the ground layer drops to zero at similar parallel and vertical field strength. Surprisingly, with both vertical and parallel magnetic fields, the ΔV_{max} drops to zero at a higher field for SQUIDs without the ground layer. Most probably vortex pinning in the ground-layer Nb film induced by the external magnetic field affects the flux modulation of the SQUID significantly. In addition, the current I_{period} in the modulation coil contributing one flux quantum as a function of magnetic field [Fig. 4(c)] shows that I_{period} drops linearly for SQUIDs with the ground layer, but stays constant for SQUIDs without the ground layer. Evidently, the superconducting properties of the ground layer are greatly affected by the magnetic field and have a strong influence on the mutual inductance between the modulation coil and the SQUID pickup loop. In feedback mode, measuring the variation of mutual inductance of the modulation coil is challenging when calibrating the exact magnetic signal during microscopy scanning.

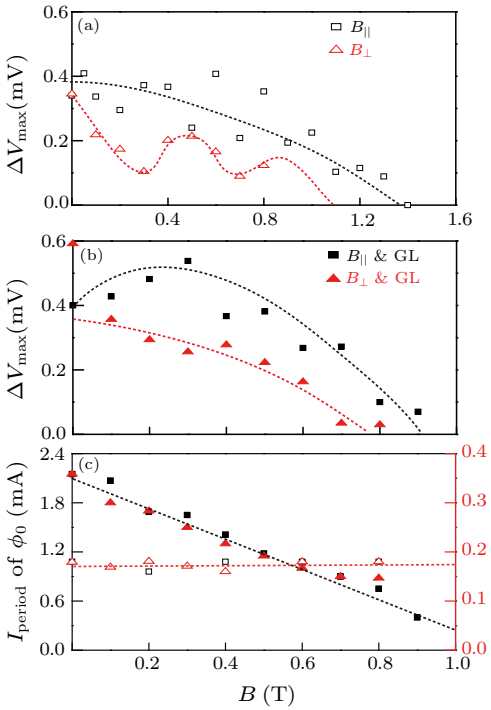

Fig. 4. Maximum swing amplitude of voltage-to-flux curve ΔV_{max} in parallel $B_{||}$ and perpendicular $B_\perp$ magnetic field with the SQUID plane of device without (a) and with (b) the ground layer. (c) Current I_{period} in the modulation coil that generates a single flux quanta in the SQUID with (solid) and without (open) the ground layer.

In conclusion, we have evaluated the performance of scanning SQUID probes that incorporate 3D nanobridge junctions. The devices show the improved magnetic modulation up to 1.4 T. The insertion of the ground layer improves the coupling symmetry of the field coil to the SQUID pick-up coil, and the modulation depth by lowering the whole inductance of the SQUID. No obvious difference arises among the four batches of devices with and without a ground layer through characterizing I_c, R_n, $dV/d\Phi$, and ΔV_{max}. We find that ΔV_{max} for all devices increases linearly with I_cR_n. However, ΔV_{max} drops to zero with smaller current values for the devices with a ground layer in both parallel and perpendicular fields. This indicates that the vortex induced by the magnetic field in the ground layer affects the performance of the SQUID. In addition, the coupling between the modulation coil and the SQUID pickup loops is also affected strongly by the magnetic field. Therefore, in the presence of a magnetic field, a scanning SQUID probe without the ground layer is more suitable for

microscopy scanning.

References

[1] Kirtley J R and Wikswo J P 1999 *Annu. Rev. Mater. Sci.* **29** 117
[2] Okayasu S, Nishio T, Ono M, Tanaka Y and Iyo A 2006 *Physica C* **437** 239
[3] Shperber Y, Vardi N, Persky E, Huber M E and Kalisky B 2019 *Rev. Sci. Instrum.* **90** 053702
[4] Cui Z, Kirtley J R, Wang Y, Kratz P A, Rosenberg A J, Watson C A, Ketchen M B and Moler A 2017 *Rev. Sci. Instrum.* **88** 083703
[5] Foroughi F, Mol J M, Müller T, Moler K A and Bluhm H 2018 *Appl. Phys. Lett.* **112** 252601
[6] Finkler A 2012 *Scanning SQUID Microscope for Studying Vortex Matter in Type-II Superconductors* (Berlin: Springer)
[7] Kirtley J R 2010 *Rep. Prog. Phys.* **73** 126501
[8] Vasyukov D, Ceccarelli L, Wyss M, Gross B, Schwarb A, Mehlin A, Rossi N, Tütüncüoglu G, Heimbach F, Zamani R R, Kovács A, Grundler D and Poggio M 2018 *Nano Lett.* **18** 964
[9] Halbertal D, Cuppens J, Shalom M B, Embon L, Shadmi N, Anahory Y, Naren H R, Sarkar J, Uri A, Ronen Y, Myasoedov Y, Levitov L S, Geim A K and Zeldov E 2016 *Nature* **539** 407
[10] Christensen D V, Frenkel Y, Chen Y Z, Xie Y W, Chen Z Y, Hikita Y, Smith A, Klein L, Pryds N and Kalisky B 2019 *Nat. Phys.* **15** 269
[11] Du J, Liu X, Qin H, Wei Z, Liu Q and Song T 2018 *Physica C* **547** 1
[12] Marguerite A, Birkbeck J, Aharon-Steinberg A, Halbertal D, Bagani K, Marcus I, Myasoedov Y, Perello D J and Zeldov E 2019 *Nature* **575** 628
[13] Uri A, Kim Y, Bagani K, Lewandowski C K, Grover S, Auerbach N, Lachman E O, Myasoedov Y, Taniguchi T, Smet J and Zeldov E 2019 *Nat. Phys.* **16** 164
[14] Chen L, Wang H, Wu L and Wang Z 2016 *Nano Lett.* **16** 7726
[15] Mizugaki Y, Yanagisawa K, Onomi T, Yamashita T, Yamamori H and Shoji A 1999 *Jpn. J. Appl. Phys.* **38** 5869
[16] Mizugaki Y, Kashiwa R, Usami K and Kobayashi T 2007 *J. Appl. Phys.* **101** 114509
[17] Pan Y P, Wang S Y, Liu X Y, Lin Y S, Ma L X, Feng Y, Chen L and Wang Y H 2019 *Nanotechnology* **30** 305303
[18] Koshnick N C, Huber M E, Bert J A, Hicks C W, Edwards H and Moler K A 2008 *Appl. Phys. Lett.* **93** 243101
[19] Fourie C J, Kunert J and Meyer H G 2013 *IEEE Trans. Appl. Supercond.* **23** 1300705
[20] Cao Y, Luo J Y, Fatemi V, Fang S, Sanchez-Yamagishi J D, Watanabe K, Kaxiras E and Jarillo-Herrero P 2016 *Phys. Rev. Lett.* **117** 116804
[21] Wang H, Yang R, Li G, Wu L, Liu X, Ren J and Wang Z 2018 *Supercond. Sci. Technol.* **31** 055015
[22] Granata C and Vettoliere A 2016 *Phys. Rep.* **614** 1
[23] Clem J R and Yang W 2011 *Nanotechnology* **22** 455501
[24] Bagani K, Sarkar J, Uri A, Rappaport M L, Zeldov E and Myasoedov Y 2019 *Phys. Rev. Appl.* **12** 044062